ECS Electrochemistry Letters, **3** (7) A72-A75 (2014)
2162-8726/2014/3(7)/A72/4/$31.00 © The Electrochemical Society

Insight into Designing High-Energy, High-Power Cathode Material for Lithium Ion Batteries

Danna Qian,[a,*] Nader M. Hagh,[b,] and Ying Shirley Meng[a,**,z]**

[a]*Department of NanoEngineering, University of California San Diego, La Jolla, California 92093, USA*
[b]*NEI Corporation, Somerset, New Jersey 08873, USA*

This work reports a physical mixture as well as an integrated composite structure (ICS) of lithium-excess layered oxides and high voltage spinel oxides. With respect to physical mixture (PM), the improvement has shown in cycling retention. Different synthesis routes would result in drastically different properties in the composite case. The optimized composite, in comparison with the non-optimized one, both energy density and the power density have increased. The optimized composite could deliver 125 mAh/g capacity after 200 cycles at a rate of 1.2 C. The work here provides some new insights into how to design better cathode materials for lithium ion batteries.
 [DOI: 10.1149/2.0061407eel]

Manuscript submitted April 25, 2014; revised manuscript received April 29, 2014. Published May 15, 2014.

Lithium ion batteries have been widely used in portable devices for the past twenty years. However, to be commercially implemented in the large-scale high-power systems such as the plug-in hybrid electric vehicle (PHEV) or plug-in electric vehicle (PEV), performance requirements are raised especially from the aspects of energy/power density, cycling life and safety issues. Therefore further improvement of LIB material and system developments are necessary. Li-excess layered oxide material is one of the best candidates for PHEVs or PEVs due to the fact that it can routinely deliver high capacities, at a voltage cut-off around 4.0 V. It suffers, however, from poor cycling performance and rate performance. Intense studies have been carried out on understanding this family of materials.[1–9] Owing to the importance of the relationship between crystal structure and electrochemical performances in lithium ion batteries, the structure of this family of materials at pristine state as well as at different states of charge have been receiving continuous attention. Despite the discrepancies in some of the observations, which may be due to the unique synthesis methods employed by various groups, great progress has generally been made on understanding and optimizing this family of compounds. To elucidate the electrochemical mechanism, oxygen activity as well as surface phase transformation have been proposed.[10–12] Optimization routes have traditionally focused on different coatings and transition metal substitutions. Recently, however, more groups have attempted to synthesize gradient as well as core-shell structures to improve performances - the core many times consisting of layered phase while the shell consists of spinel phase.[13–16]

In this study, different approaches have been adopted to improve the performance of the Li-excess layered oxide material, including making physical mixtures with high voltage spinel ($LiNi_{0.5}Mn_{1.5}O_4$) as well as making the composite of layer and spinel structures. High voltage spinel was designed to improve both the voltage and rate performance of the Li-excess material, as well as to make up the irreversible capacity for Li-excess in a full cell. The materials were characterized by X-ray diffraction (XRD) and scanning electron microscope (SEM); their electrochemical performances, including cycling and rate, were compared. Physical mixture with high voltage spinel was shown to not only improve the cycling, but also the rate capability as well. By optimizing the synthesis methods of the composite, remarkable improvements in energy and power can be achieved.

Experimental

Materials.— All samples were synthesized by NEI Corporation. The composition of the layer-layer (LL) was $Li[Li_{0.2}Mn_{0.53}Ni_{0.13}Co_{0.13}]O_2$, and the physical mixture (PM) was designed to be 15 wt% of $LiMn_{1.5}Ni_{0.5}O_4$ and 85 wt% of the LL phase physically mixed together. The composite synthesized by solid-state method (LS_SS) adopts the formula of $Li_{1.2}Ni_{0.25}Mn_{0.75}O_2$; the composite synthesized using wet chemistry will be referred to as LS_WC for short.

Materials characterization.— The particle morphology and size distribution of the synthesized powders were determined using an FEI XL30UHR SEM (ultra high resolution SEM) with a Sirion column, which enables very high resolution imaging at low kV. All images were collected under an accelerating voltage of 10 kV. The powders were suspended on double-sided carbon tape, placed on a specimen holder.

XRD spectra were taken using a Bruker D8 advance diffractometer with a Bragg Brentano theta-2theta geometry and a Cu Kα source. Samples were scanned from 10° to 80° with a scan rate of 0.025°per second.

Electrochemical characterization.— Cathodes were prepared by mixing 80 wt% active material with 10 wt% acetylene carbon black (99.9%) and 10 wt% poly (vinylidene fluoride) in *N*-methyl pyrrolidone solution. The slurry was cast onto Al foil using a doctor blade and dried overnight in a vacuum oven at 80°C. The electrode disks were punched and dried again at 80°C for 6 h before storing them in an argon-filled glove box (H_2O level of <1 ppm). 2016 type coin cells were used to study the electrochemical behavior of the compounds. Lithium metal ribbon and 1 M$LiPF_6$ in a 1:1:1 EC: DMC: DEC solutions were used as anode and electrolyte, respectively. A Celgard model C480 separator (Celgard Inc.) was used as the separator. The coin cells were assembled in the same argon-filled glove box and tested on an Arbin battery cycler in galvanostatic mode. The cycling tests were conducted between 2.0 V and 4.8 V for the LL & PM, while 2.0 V –5.0 V for LS_SS and LS_WC; 170 mA/g was used as 1C rate. The loading density for the rate performance is around 4 mg/cm^2 except for LS_SS sample, which was around 10 mg/cm^2.

Results and Discussion

Physical mixing of layer and spinel.— SEM images of the four samples are shown in Figure 1, 1a to 1c for LL, and 1d to 1f for PM. The primary particle size of LL is around 100 nm – 200 nm, while there is no uniform secondary particle size. In the PM sample, it is clear that two different morphologies co-exist; where the spinel phase has primary particle size around 1 micron and the morphology is more faceted than the layered phase.

The XRD of the LL and PM are plotted in Figure 2. As labeled out, besides the layered characteristic peaks, the PM also contains the spinel phase. The detailed two-phase refinement of the PM is shown in Figure S1. Two phases are adopted in the refinement as LL ($Li[Li_{0.2}Mn_{0.53}Ni_{0.13}Co_{0.13}]O_2$) and spinel ($LiMn_{1.5}Ni_{0.5}O_4$). It shows that from the refinement, the weight percentage of the two phases is

*Electrochemical Society Student Member.
**Electrochemical Society Active Member.
zE-mail: shirleymeng@ucsd.edu

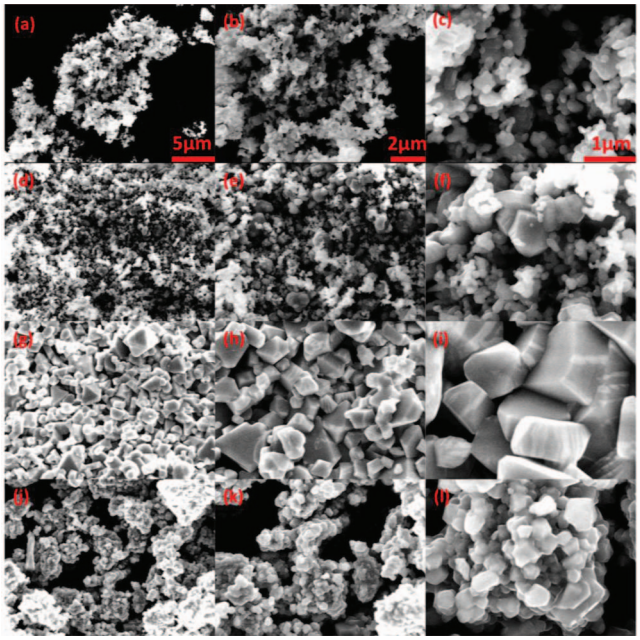

Figure 1. SEM images of LL (a) - (c), PM (d) - (f), LS_SS (g) - (i), LS_WC (j) - (l) at different magnifications. The scale bar is the same for each column.

85% and 15%, respectively (detailed refinement parameters in Table S1). From the ICP results, the mole ratio is accurate as what was designed.

The electrochemical performances between LL and PM are compared in Figure 3, which shows the first 10 cycles of each material (3a LL, and 3b PM), at a rate of 17 mA/g. Figure 3c and 3d show a detailed capacity comparison in terms of both cycling and rate capability. By comparing the voltage profile of LL and PM, they show similar plateau around 4.5 V, which is well known for Li-excess material. PM shows a small plateau around 2.5 V at discharge, however, which is representative of the activation of part of the spinel phase. The first cycle irreversible capacity is 97 mAh/g and 79 mAh/g for LL and PM materials, respectively. Subsequent LL cycles consistently show 10–15 mAh/g of irreversible capacity, while PM capacity retention was much improved. The columbic retention after 10 cycles is 85% and almost 100% for LL and PM materials, respectively. Contrary to our expectations, LL material showed better rate performance than PM, from C/10 to 2C. This is mainly because the initial capacity of LL was higher than PM. Rates higher than 2C were not tested, but from the trend indicated in Figure 3d, at faster rates, e.g. 10C, PM material may deliver larger capacities compared to LL material. In summary, the cycling retention can be improved by physical mixing LL with spinel. Future work on the influence of activating more spinel in the material will be investigated.

Making layer and spinel into composite.— As shown in the previous section, by physically mixing layer and spinel phase, the first cycle irreversible capacity can be reduced and the cycling retention can be increased. It is proposed that making layer and spinel into a composite may further improve the performances.

The SEM images of LS_SS ((g) - (i)), and LS_WC ((j) - (l)) are shown in Figure 1. The primary particles of LS_SS more closely resemble the spinel phase, with the size of several microns. By changing the synthesis method but maintaining the same designed stoichiometry, the primary particle size of LS_WC was much reduced, from 1 μm to 500 nm. Using ICP-OES, the stoichiometry of LS_SS material was determined to correlate with its designed target, while LS-WC material contained extra Li with unknown reason from wet synthesis.

The XRD of LS_SS material shown in Figure 2 suggests it consists of both layer and spinel phases, based on the appearance of doublet peaks. On the other hand, LS_WC material shows only single peaks, which can be perfectly fit to a layered structure with larger d spacings. However, from the electrochemical voltage profile, plotted in Figure S2, with higher charging plateau compared to LL, it is believed that there is existence of composite and uniformly distributed layer and spinel phases that result in clean XRD patterns.

The electrochemical performances of these two materials were compared in Figure 4. As shown in Figure 4a, the orange arrow points toward increasing cycle numbers for LS_SS; the cycling rate was 8.5 mA/g. The capacity of LS_SS material was shown to increase upon cycling, evidence of so-called "activation", which proceeds to high capacities. The non-uniform TM distributions as well as the large particle size (Figure S3) was the main reason contributing to the activation process. Rate testing was performed after activation (four cycles at 8.5 mA/g), as shown in Figure 4b. This figure shows that LS_SS material can deliver up to 118 mAh/g at a rate of C/2.

In contrast to LS_SS material, LS_WC, with a much smaller particle size, was shown to deliver higher capacity and better cycling retention. The long plateau at 4.9 V in Figure 4c is believed to be due to a combination of side-reaction and the presence of extra Li. The rate performance demonstrated in Figure 4d shows that a capacity of 160 mAh/g can be achieved at a rate of 2C. Long-term cycling performance shown in Figure 4e was carried out at C/8 for the first six cycles, and 1.2C for both charge and discharge at the following cycles, the material is able to deliver around 125 mAh/g after 200 cycles.

General discussions.— Our approach to realize high power and high energy density materials was presented by physically mixing

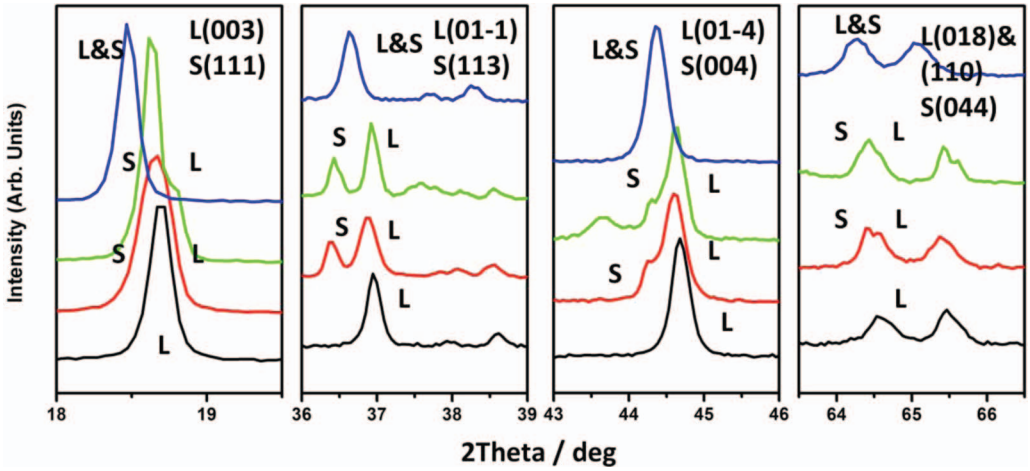

Figure 2. XRD spectra of LL (black), PM (red), LS_SS (green) and LS_WC (blue).

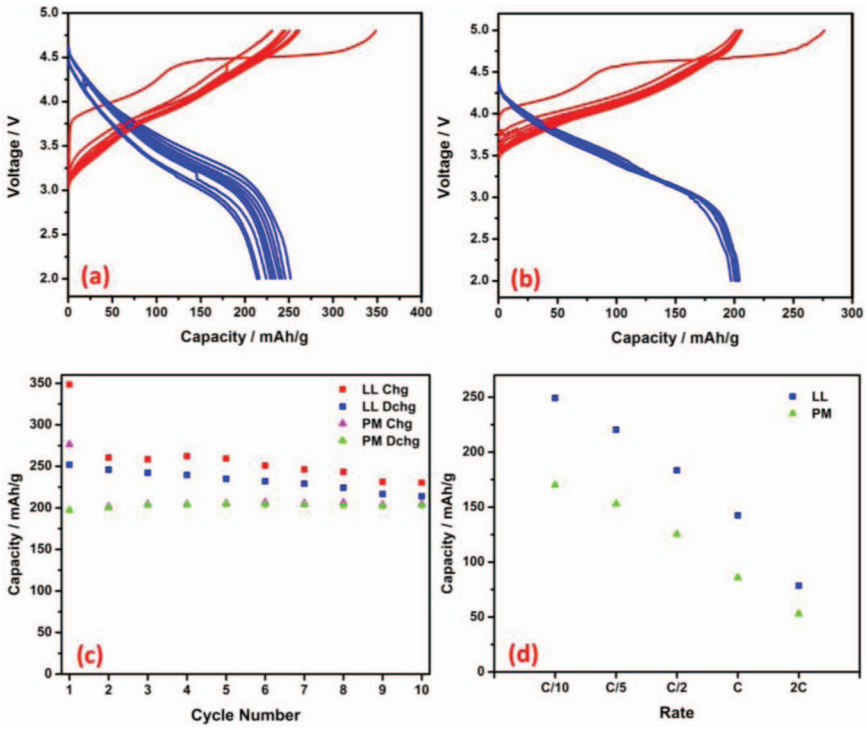

Figure 3. Electrochemical performance of LL and PM. (a) LL at 17 mA/g for 10 cycles, (b) PM at 17 mA/g for 10 cycles, (c) cycling comparison, (d) rate comparison.

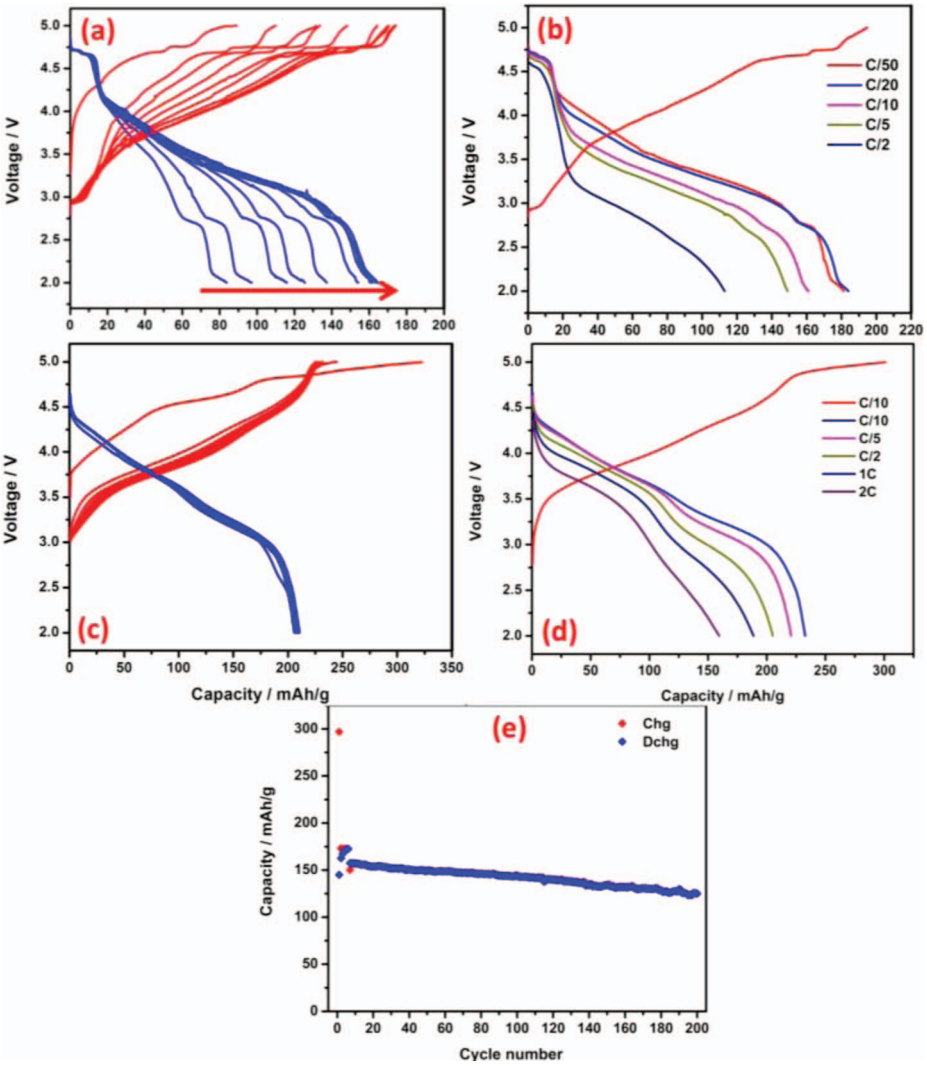

Figure 4. Electrochemical performance of LS_SS and LS_WC. Cycling (a) and rate (b) of LS_SS; cycling (c) and rate (d) of LS_WC, (e) 250 mA/g cycling of LS_WC.

Li-excess (high capacity) and high voltage spinel phase (high power) materials, as well as making integrated composite structures. Both of the layered and spinel phases consist of oxygen cubic close-packed frameworks, which make them structurally compatible. Physical blending can improve the first cycle irreversible capacity and cycling retention to a certain degree, as shown in our results. It would not, however, solve the intrinsic structure problem in Li-excess materials upon cycling. In addition, how to activate all spinel phase in the physical mixture still requires further studies. By making spinel into layered structure forming composite, as shown, the performance can be further improved with smaller voltage depression upon cycling (Figure S4); a detailed mechanistic study is still underway. It shows by carefully engineering, layer-spinel composite can provide high energy high power material with long cycle life as well as possibly improve the voltage stability.

Conclusions

In this study, we have obtained new electrode materials by both making physical mixture and composite structures with Li-excess and spinel structures, in order to improve the electrochemical performances of pure Li-excess layered oxide materials. The composite synthesized by wet chemistry method gives the best results, with a capacity of 125 mAh/g delivered after 200 cycles, at a rate of 1.2 C. More in-depth studies on the mechanism will be carried out in future work.

Acknowledgment

The authors thank the funding through NASA SBIR/STTR program under contract number NN10CB59C. D. Q. acknowledge the precious discussion with Dr. Ganesh Skandan and the assistance from Mr. Haodong Liu.

References

1. Z. Lu and J. R. Dahn, *Journal of the Electrochemical Society*, **149**, A815 (2002).
2. Y. J. Park, Y.-S. Hong, X. Wu, K. S. Ryu, and S. H. Chang, *J. Power Sources*, **129**, 288 (2004).
3. A. D. Robertson and P. G. Bruce, *Electrochemical and Solid-State Letters*, **7**, A294 (2004).
4. Y. S. Meng, G. Ceder, C. P. Grey, W. S. Yoon, M. Jiang, J. Breger, and Y. Shao-Horn, *Chem. Mater.*, **17**, 2386 (2005).
5. M. M. Thackeray, S.-H. Kang, C. S. Johnson, J. T. Vaughey, R. Benedek, and S. A. Hackney, *Journal of Materials Chemistry*, **17**, 3112 (2007).
6. S. H. Kang and M. M. Thackeray, *Journal of the Electrochemical Society*, **155**, A269 (2008).
7. M. Jiang, B. Key, Y. S. Meng, and C. P. Grey, *Chem. Mat.*, **21**, 2733 (2009).
8. C. R. Fell, K. J. Carroll, M. Chi, and Y. S. Meng, *Journal of the Electrochemical Society*, **157**, A1202 (2010).
9. B. Xu, C. R. Fell, M. Chi, and Y. S. Meng, *Energy and Environmental Science*, **4**, 2223 (2011).
10. B. Xu, C. R. Fell, M. Chi, and Y. S. Meng, *Energy and Environmental Science*, **4**, 2223 (2011).
11. C. R. Fell, D. Qian, K. J. Carroll, M. Chi, J. Jones, and Y. S. Meng, *Chem. Mater.* 2013.
12. K. J. Carroll, D. Qian, C. Fell, S. Calvin, G. M. Veith, M. Chi, L. Baggetto, and Y. S. Meng, *Phys. Chem. Chem. Phys.* 2013.
13. C. S. Johnson, N. Li, J. T. Vaughey, S. A. Hackney, and M. M. Thackeray, *Electrochem. Commun.*, **7**, 528 (2005).
14. J. Cabana, C. S. Johnson, X. Q. Yang, K. Y. Chung, W. S. Yoon, S. H. Kang, M. M. Thackeray, and C. P. Grey, *J. Mater. Res.*, **25**, 1601 (2010).
15. Y. Cho, S. Lee, Y. Lee, T. Hong, and J. Cho, *Advanced Energy Materials* 2011, n/a.
16. E.-S. Lee, A. Huq, H.-Y. Chang, and A. Manthiram, *Chem. Mater.* 2012.